Available online at www.sciencedirect.com

SCIENCE DIRECT

Diamond & Related Materials 14 (2005) 714–718

DIAMOND AND RELATED MATERIALS

www.elsevier.com/locate/diamond

Growth and field emission properties of small diameter carbon nanotube films

Y.Y. Wang[a,*], S. Gupta[a], J.M. Garguilo[a], Z.J. Liu[b], L.C. Qin[b], R.J. Nemanich[a]

[a]North Carolina State University, Department of Physics, Raleigh, NC 27695-8202, USA
[b]University of North Carolina, Chapel Hill, Department of Physics and Astronomy, Chapel Hill, NC 27599-3255, USA

Available online 8 December 2004

Abstract

Vertically aligned carbon nanotube films with diameters smaller than 5 nm, high densities up to $10^{12}/cm^2$, and lengths of ~ 5–8 μm were deposited by microwave plasma-assisted chemical vapor deposition. Experiments show that, by continuous reduction in the thickness of the iron film (i.e., ~0.3–0.5 nm), small diameter carbon nanotubes can be achieved with diameters that ranged from 1–5 nm, and the films are comprised of both single- and double-wall nanotubes. The electron field emission properties of the films were investigated by variable distance field emission and temperature-dependent field electron emission microscopy (T-FEEM). The films showed an emission site density of $\sim 10^4/cm^2$ and a threshold field of 2.8 V/μm similar to multiwalled nanotubes (1.9 V/μm). In addition, they also exhibited a temperature dependence of the emission site intensity.

Keywords: Small diameter carbon nanotubes; MWCVD; Growth; Field emission

1. Introduction

Single- or double-wall carbon nanotubes (CNT) with small diameters ranging from 1–5 nm can be either semiconducting or metallic. They also exhibit a high aspect ratio, chemical and environmental stability, and robust mechanical properties, which make them ideal candidates as components of nanodevices [1,2]. Methods such as dc electric arc discharge (EA) [3] and pulsed laser vaporization (PLV) [4] have been used to grow single-wall nanotubes (SWNTs), but the products are powders with tangled nanotubes and significant catalyst impurities. Recently, thermal chemical vapor deposition (CVD) has been employed to obtain well-separated individual tubes on flat substrates or suspended across trenches [5]. Nevertheless, vertically aligned films are still preferred in the fabrication of nanotube-based field emission devices. In prior studies, several research groups have shown that microwave plasma CVD (MWCVD) growth results in vertically aligned nanotube films, which has been attributed to the field at the edge of plasma sheath [6]. However, multiwalled CNT (MWNT) with bamboo-like structure are mostly obtained with this approach [7,8]. In this study, we employed thin Fe catalyst layers (<1 nm), elevated growth temperatures (~850 °C), and relatively short growth time (<40 s) with acetylene and ammonia gas mixtures to achieve well-crystallized small diameter nanotubes (<5 nm) with reduced amorphous carbon and impurity content.

To successfully fabricate CNT-based field emission devices, it is necessary to understand their field emission properties. In this context, it is desirable to be able to characterize spatially the origin of the emission. Several research groups have studied the field emission properties from both single-wall and multiwalled carbon nanotubes in all forms (individual, mat, and vertically aligned) using traditional emission current-applied voltage (I–V) characterization and field emission energy distribution (FEED) [9,10]. In this study, we employed variable distance field emission [11] and field electron emission microscopy

* Corresponding author. Tel.: +1 919 515 2474; fax: +1 919 515 7331.
E-mail address: ywang10@unity.ncsu.edu (Y.Y. Wang).

0925-9635/$ - see front matter © 2004 Elsevier B.V. All rights reserved.
doi:10.1016/j.diamond.2004.10.003

(FEEM) at elevated temperatures (T-FEEM) to characterize the field emission properties of nanotubes. Furthermore, high-temperature thermionic electron emission from carbon nanotubes has been carried out with a perspective of developing direct thermal-to-electrical power conversion applications [12,13].

2. Experimental procedures

The carbon nanotubes films were grown in a 1.5 kW IPX3750 ASTEX microwave chemical vapor deposition reactor, which has also been employed to grow micro and nanocrystalline diamond films [14]. Initially, Si (001) (n^+-type) substrates were thermally oxidized, and an iron layer with thickness of 5 and 0.5 nm as catalyst was deposited using electron beam evaporation. An SiO_2 layer (30–180 nm) was used as a diffusion barrier preventing Fe diffusion into Si and the formation of a silicide. Before deposition, the as-prepared substrates ($Fe/SiO_2/Si$) were annealed in vacuum (~10^{-8} Torr) at ~850 °C for 10 min to promote the formation of discrete Fe droplets/islands. These annealed substrates were then introduced into the MWCVD reactor, which was evacuated to a base pressure <10^{-3} Torr. A gaseous mixture of ammonia and acetylene was admitted with flow rates of 70 and 18 sccm, respectively. The chamber pressure was maintained at 20 Torr during the deposition, and the deposition temperature of ~850 °C was achieved through induction heating of the substrate combined with the MW power source of 600 W. Growth continued for ~30–90 s. The nanotube film growth was carried out in a configuration where the substrates were partially covered with sections of a Si wafer which served to screen the actual substrates from the plasma, and the deposition took place underneath the covered regions.

As-deposited CNT samples were characterized using scanning electron microscopy (SEM), high-resolution transmission electron microscopy (HRTEM), and Raman spectroscopy (RS). SEM images were obtained using a JEOL 6400 with beam energy of 5 KV. HRTEM was performed on a JEOL 2010F microscope operating at 200 KV. The samples for HRTEM were prepared by sonicating a small amount of the peeled CNTs in methanol for 15 min and drying a few drops of the suspension on a holey-carbon or Cu grid.

Variable distance field emission was conducted in vacuum (~3×10^{9} Torr). A voltage sweep from 0 to 1100 V was applied to the anode, and current–voltage curves were recorded with different distances between the anode and the sample, where the distance (d) is controlled by a PRI stepping motor controller (Model SK-1). The photoelectron emission and field electron emission microscopy (PEEM and FEEM) measurements were performed in an Elmitec UHV-photo electron emission microscope (Model PEEM III) with a base pressure of ~10^{-10} Torr. The system has sample heating, which was used to degas the sample surface at 150 °C and to obtain temperature-dependent field emission microscopy (T-FEEM) measurements. The field of view was varied between 150 and 2 μm with a resolution of <15 nm at the highest magnification. For all of the imaging measurements, a high voltage of 20 kV is applied between the anode and the cathode with a nominal separation of 3–4 mm, which results in an applied field of ~5 V/μm.

3. Results and discussion

3.1. Growth of small diameter carbon nanotubes

Fig. 1a shows a representative scanning electron microscopy image of the as-grown carbon nanotubes films on annealed 0.5 nm Fe catalyst layers. The image displays a high areal density (~10^{12}/cm^2) of long fine tubes, which are aligned perpendicular to the substrate. The length of the nanotubes was ~4 μm, obtained with the short deposition times of <30s resulting in a growth rate of ~0.13 μm/s. This growth rate is significantly greater than the ~0.08–0.10 μm/s reported by other groups using plasma enhanced CVD

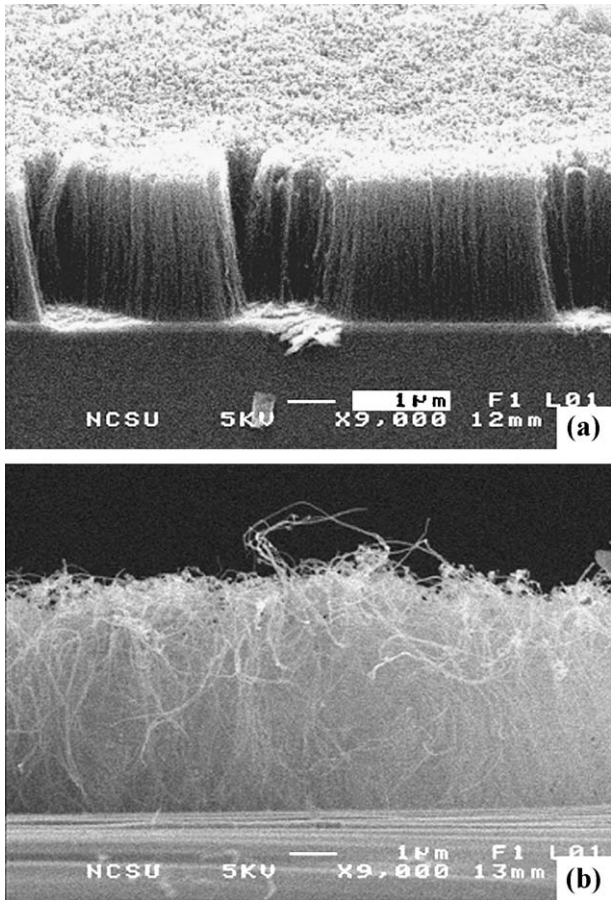

Fig. 1. SEM images of MWCVD carbon nanotubes films on (a) 0.5- and (b) 5-nm Fe catalyst.

techniques [6,15] and for multiwalled carbon nanotubes (~0.01 μm/s) in our previous work [16]. Fig. 1b displays an SEM image of a nanotube film grown on a 5-nm Fe layer. The film has a thickness of ~4 μm and is not as well aligned as the 0.5-nm Fe sample.

High-resolution TEM images shown in Fig. 2a and b exhibit the presence of single and double-wall carbon nanotubes (S/DWNT) grown on 0.5-nm Fe. These results are also supported by Raman measurements [17]. The tubes were either isolated or weakly bundled. The diameters for most of the isolated nanotubes ranged between 0.8–1.25 and 4.0–5.0 nm for single- and double-walled nanotubes, respectively (see Fig. 2a). The observation of closed nanotubes with no catalyst at the tip indicates that the base growth model is predominant in our system [17]. We speculate that the relatively smaller catalyst size and the higher deposition temperature enhance anchoring of the catalyst and promote base growth. Fig. 2b and c shows HRTEM images of the nanotubes grown on the 5-nm Fe. Fig. 2b shows a tube with ~12 walls and a diameter of ~15 nm, while Fig. 2c displays a tube with ~30 walls and a diameter of ~30 nm. Compared to the small diameter nanotubes, the MWNTs normally have a wide range of diameters which is most likely related to a large island/droplet size distribution for the thicker Fe layer.

We have previously proposed a growth model to describe the function of catalyst size in terms of carbon surface and bulk diffusion [18]. Briefly, the origin of the internal structure of nanotubes (bamboo-like or fiber-like) is ascribed to bulk diffusion, while surface diffusion is apparently the major contribution for wall formation. The ratio between surface and bulk diffusion rates will affect the internal structure of the CNTs (hollow, bamboo-like, and fiber-like). To maintain the catalyst droplets activated without being poisoned by a-C, short time deposition and ammonia etching are important approaches. It has been proposed that one of the primary functions of ammonia is to etch competing graphitic or amorphous carbon deposits [19].

3.2. Field emission of small diameter nanotube films

Variable distance field emission measurements were made on both nanotube films. Fig. 3a shows I–V curves at various anode–cathode (sample) distances for nanotubes grown on 0.5-nm Fe (the change of distance between each curve is 27.5 μm). All curves exhibit exponential characteristics typical of field emission. By noting the voltage at a current of 1 nA from each I–V curve and the corresponding distance (d), a plot of V–d can be obtained. The slope of the V–d trend line represents the threshold field for 1 nA of emission current, which is shown in Fig. 3b. For comparison, the multiwalled nanotube film with Fe thickness of 5 nm is also shown. From V–d plots, a threshold field of 2.8 V/μm is obtained for the small diameter NTs, while the threshold field for the MWNTs is 1.9 V/μm. The single- and double-wall CNT film grown on the 0.5-nm Fe film is a

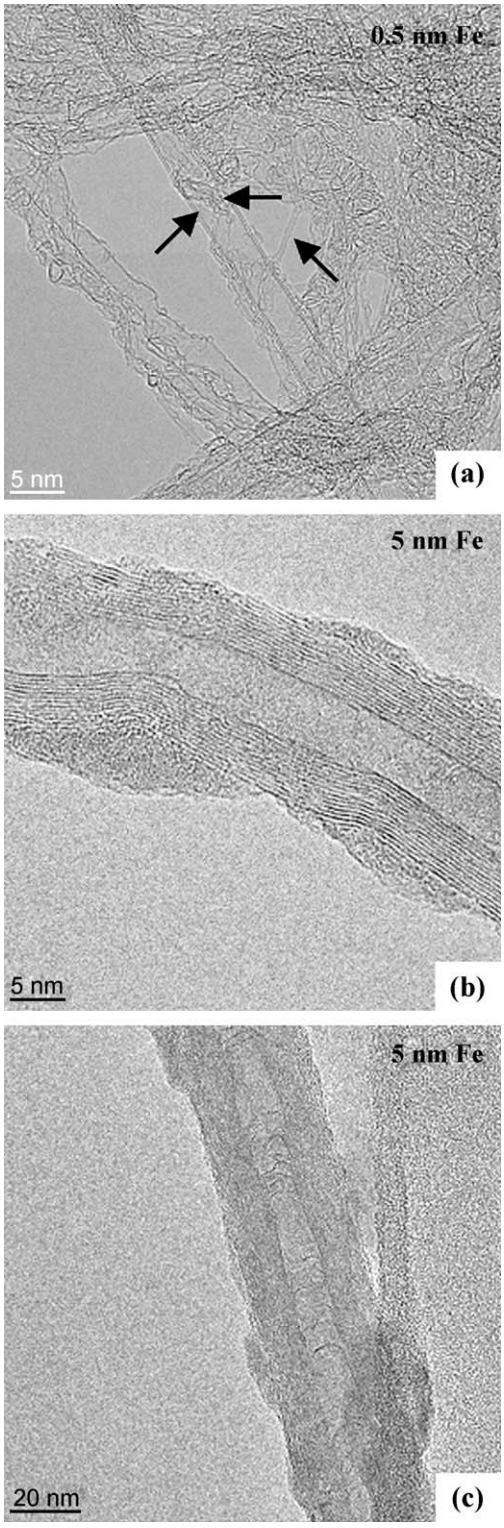

Fig. 2. High-resolution transmission electron microscopy (HRTEM) images of MWCVD carbon nanotubes. Panel (a) shows well-graphitized double- and single-wall carbon nanotubes grown on 0.5-nm Fe marked by arrows. Panels (b) and (c) show both hollow and bamboo-like internal structure of the multiwalled nanotubes grown on 5-nm Fe.

mixture comprised of semiconducting and metallic tubes, and it appears that the field emission of this mixture are not pronouncedly different from MWNTs which are totally metallic. Although the small diameter nanotubes have a higher aspect ratio (length/radius) compared to the MWNTs, the high areal density of small diameter films (10^{12}/cm^2) may lead to strong electrostatic screening [20]. It should also be noted that both films were grown with a SiO_2 diffusion layer, which can limit the field emission current due to a larger resistance.

To investigate the temperature dependence of the field emission properties of these nanotube films, field emission microscopy measurements were initiated as a function of temperature (T-FEEM). The sample (0.5-nm Fe) was first measured at RT, and short-term fluctuations (or drifts) were observed on the order of 6–8%, which may be due to adsorbate interactions on the nanotubes. The temperature was then ramped up to 900 °C (shown in up-sweep in Fig. 4). Increasing the sample temperature results in minimal change in the emission site structure or pattern, and the nanotubes showed increased emission site intensity. When the temperature is ramping up, an increase of chamber pressure from 1×10^{9} to 4.5×10^{9}Torr is observed, which may affect the emission from the CNTs (it should be noticed that at 600 °C, the channel plate voltage, which controls amplification of image intensity, was reduced from 1.25 to 1.15 KV to protect the channel plate). A down sweep was initiated after the temperature was ramped to 1000 °C. The images show a decreasing emission site intensity. During ramping down, the pressure is very stable at ~2×10^{9} Torr, and the down sweep of the T-FEEM is most likely attributed to a thermionic contribution to the field emission.

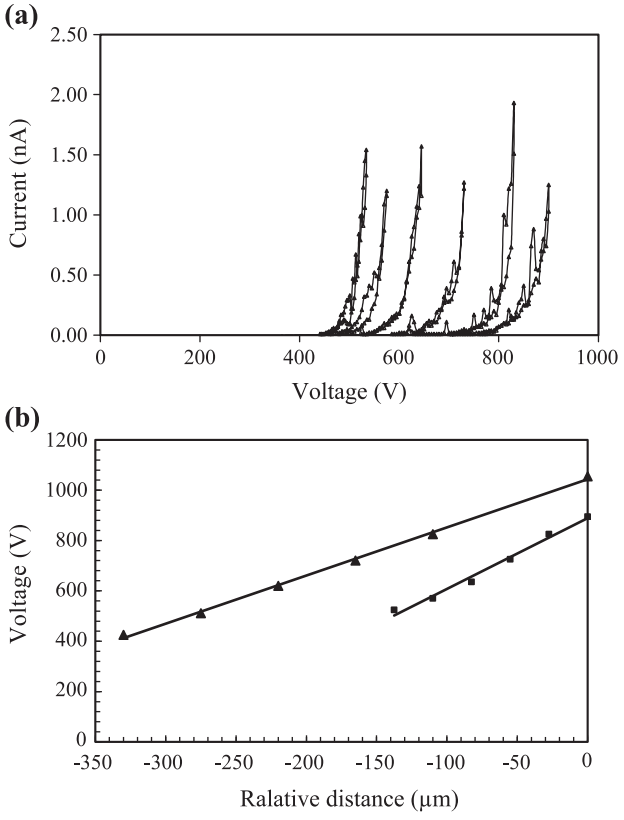

Fig. 3. Panel (a) shows variable distance field emission measurements of a nanotube films (0.5-nm Fe). The distance between each I–V curve is 27.5 μm. Panel (b) shows a plot of voltage–distance dependence for field emission current of 1.0 nA (the upper line is for NTs with 5-nm Fe and the lower line is for NTs with 0.5-nm Fe).

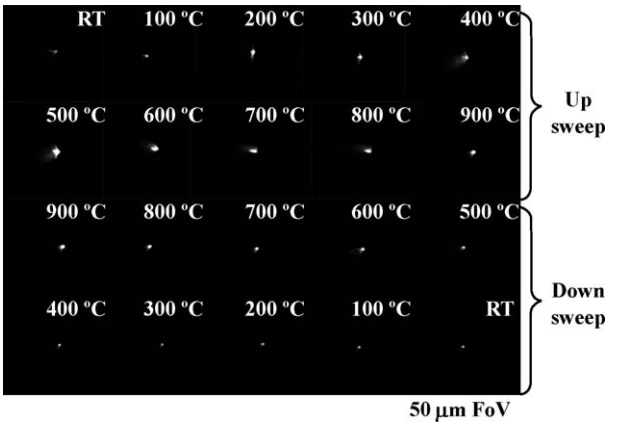

Fig. 4. Temperature-dependent field emission imaging for a small diameter nanotube film grown on 0.5 nm Fe for both warming up and cooling down cycle. During up-sweep, the channel plate voltage, which controls amplification of image intensity, was reduced at 600 °C from 1.25 to 1.15 KV to protect the channel plate.

4. Conclusions

In conclusion, we have presented a way of depositing aligned single- and double-wall carbon nanotubes by microwave plasma-assisted CVD with a C_2H_2/NH_3 gas mixture. By using elevated substrate temperatures and effective manipulation of the Fe catalyst thickness and hence improving catalyst efficiency, the growth characteristics of the nanotubes were considerably affected. As a result, we were able to grow well-graphitized, vertically aligned small diameter carbon nanotubes. Both variable distance field emission and T-FEEM measurements were carried out on small diameter nanotubes, and they show similar threshold field to the MWNTs. The emission characteristics at elevated temperatures indicate a thermionic contribution to the field emission, which may be important for the application of carbon nanotube-based field emitters in cathodes and thermionic energy converters.

Acknowledgements

We gratefully acknowledge Duke University Free Electron Laser Laboratory where all of the photo and field electron emission microscopy experiments were performed. This research is supported in part by the TEC ONR–MURI and the Department of Energy Center–Argonne National Laboratory Grants.

References

[1] M.S. Dresselhaus, G. Dresselhaus, P. Avouris, Carbon Nanotubes: Synthesis, Structure, and Application, Springer, Berlin, 2001.
[2] Ph. Avouris, Science 292 (2001) 705.
[3] C. Journet, W.K. Maser, P. Bernier, A. Loiseau, M. Lamy de la Chapelle, S. Lefrant, P. Deniard, R. Lee, J.E. Fischer, Nature 388 (1997) 756.
[4] A. Thess, R. Lee, P. Nikolaev, H. Dai, P. Petit, J. Robert, C. Xu, Y.H. Lee, S.G. Kim, A.G. Rinzler, D.T. Colbert, G.E. Scuseria, D. Tomanek, J.E. Fischer, R.E. Smalley, Science 273 (1996) 483.
[5] S. Huang, A.W.H. Mau, T.W. Turney, P.A. Whit, L. Dai, J. Phys. Chem., B 104 (2000) 2193.
[6] C. Bower, W. Zhu, S. Jin, O. Zhou, Appl. Phys. Lett. 77 (2000) 830.
[7] R.G. Lacerda, A.S. Teh, M.H. Yang, K.B.K. Teo, N.L. Rupesinghe, S.H. Dalal, K.K.K. Koziol, D. Roy, G.A.J. Amaratunga, W.I. Milne, M. Chhowalla, D.G. Hasko, F. Wyczisk, P. Legagneux, Appl. Phys. Lett. 84 (2004) 269.
[8] Y.J. Yoon, J.C. Bae, H.K. Baik, S.J. Cho, Se-Jong Lee, K.M. Song, N.S. Myung, Physica B 323 (2002) 318;
H.B. Peng, T.G. Ristroph, G.M. Schurmann, G.M. King, J. Yoon, V. Narayanamurthi, J.A. Golovchenko, Appl. Phys. Lett. 83 (2003) 4238.
[9] W.B. Choi, D.S. Chung, J.H. Kang, H.Y. Kim, Y.W. Jin, I.T. Han, Y.H. Lee, J.E. Jung, N.S. Lee, G.S. Park, J.M. Kim, Appl. Phys. Lett. 75 (1999) 3129.
[10] O. Gröning, O.M. Kuttel, Ch. Emmenegger, P. Gröning, L. Schlapbach, J. Vac. Sci. Technol., B 18 (2000) 665.
[11] A.T. Sowers, B.L. Ward, S.L. English, R.J. Nemanich, J. Appl. Phys. 86 (1999) 3973.
[12] F.A.M. Koeck, J.M. Garguilo, R.J. Nemanich, Diamond Relat. Mater. 13 (2004) 2052.
[13] S.H. Shih, T.S. Fisher, D.G. Walker, A.M. Strauss, W.P. Kang, J.L. Davidson, J. Vac. Sci. Technol., B 21 (2003) 587.
[14] F.A.M. Köck, J.M. Garguillo, R.J. Nemanich, S. Gupta, B.R. Weiner, G. Morell, Diamond Relat. Mater. 12 (2003) 474.
[15] W. Kim, H.C. Choi, M. Shim, Y. Li, D. Wang, H. Dai, Nano Lett. 2 (2002) 703.
[16] Y.Y. Wang, F.A.M. Kock, J.M. Garguilo, R.J. Nemanich, Diamond Relat. Mater. 13 (2004) 1287.
[17] Y.Y. Wang, S. Gupta, R.J. Nemanich, Appl. Phys. Lett. 85 (2004) 2601.
[18] Y.Y. Wang, S. Gupta, R.J. Nemanich, J. Appl. Phys. (submitted).
[19] M. Chhowalla, K.B.K. Teo, C. Ducati, N.L. Rupesinghe, G.A.J. Amaratunga, A.C. Ferrari, D. Roy, J. Robertson, W.I. Milne, J. Appl. Phys. 90 (2001) 5308 (and references therein).
[20] L. Nilsson, O. Groening, C. Emmenegger, O. Kuettel, E. Schaller, L. Schlapbach, H. Kind, J.-M. Bonard, K. Kern, Appl. Phys. Lett. 76 (2000) 2071.